the bounding streamline of the airfoil/wake (see Fig. 1). The describing equations are as follows:

$$F(w) = \tfrac{1}{2}(w - u_s)^2 = \varphi + i\psi \tag{1}$$

$$z(w) = \int_0^w (w' - u_2)^{k_2}(w' - u_3)^{k_3} \ldots (w' - u_n)^{k_n}\, dw' \tag{2}$$

$$k_i = \text{angle change}/\pi$$

$$F(z) = F[w(z)] \tag{3}$$

$$\bar{V}/V_\infty = dF/dz = V_x/V_\infty - iV_y/V_\infty \tag{4}$$

$$C_p = (p - p_\infty)/\tfrac{1}{2}\rho V_\infty^2 = 1 - (V/V_\infty)^2 \tag{5}$$

It is necessary to specify the forward stagnation point on the underside of the airfoil. Examination of pressure distribution data suggests the location 2% chord, for cases in which the separation is near the leading edge.

The chief difficulty in using the transformation is that the deeply embedded parameters $u_2, u_3, \ldots, u_n$ in Eq. (2) must be obtained by some iterative procedure based on matching the "vertex" coordinates $z_2, z_3, \ldots, z_n$. This is done through a complex arithmetic, double precision FORTRAN routine for the IBM 360, written by the author. Numerical quadrature of the complex integrand in Eq. (2), taking proper account of the (integrable) singularities, yields a z_i set for any u_i set. This calculated z_i set is compared with the inputted (z_i) geometry, and the first-order, multivariable Newton's method[4] is used to generate a set of Δu_i corrections. The process can be made to converge with arbitrary accuracy. The substance of this work, therefore, is the application of current electronic computer capabilities to an established, general mathematical method.

Each concave corner is a stagnation point and each convex corner is a point of infinite velocity, in perfect fluid theory. However, calculation of pressure distributions by Eqs. (4) and (5) shows that these singularities are important only locally and their effects may be smoothed over or ignored.

The round cylinder without circulation provides a standard test for any perfect fluid calculation method. The geometry of the infinitesimal "wake" and the location of the forward stagnation point are determined by symmetry. Figure 2 shows the result of applying the present program to the purposely crude polygonal approximation as drawn, compared with the well-known solution[5]:

$$C_{p_{cyl}} = 1 - 4\sin^2\beta \tag{6}$$

It is seen that the computer answer does agree with the standard solution on the average (and oscillates about it).

Little test data including both stalled airfoil pressure distributions and the corresponding wake geometry are found in the literature. However, Fig. 3 shows a comparison between calculated answers and pressure measurements found in Ref. 6. Agreement is no better than fair. The near wake form was taken from a sketch in that report, which was generated from two locus points of "definite turbulence" as indicated by fine threads on movable wire probes. In addition to the questionable accuracy of the wake geometry, it is specifically noted in Ref. 6 that model blockage effects caused the upper surface C_p measurements to be more negative than they would have been in free air. It is not possible at this time to weigh the imprecision of the experiment against the error incurred by the use of the idealized wake model.

Experimental measurement of at least gross wake geometry and separated airfoil pressure distributions would be very helpful. This information, together with rates of dynamic pressure recovery in the unsymmetrical near wake, is also needed for systematic study of T-tail deep stall.

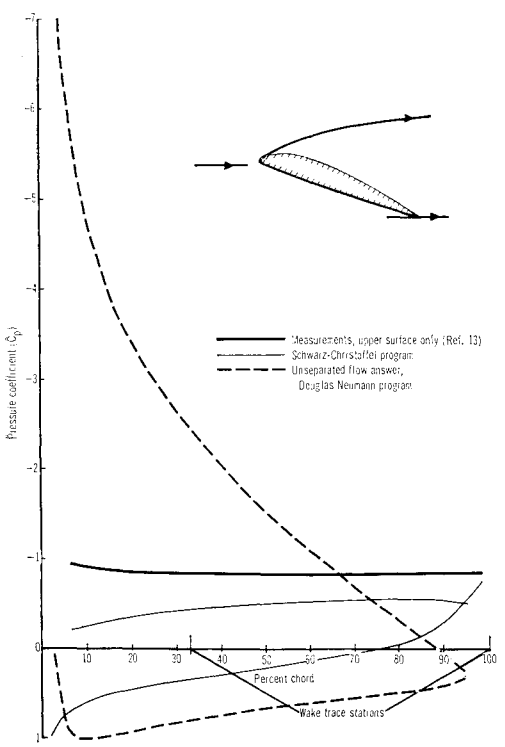

Fig. 3 Pressure distribution on English Aircrew 4 at 19° incidence.

References

[1] Giesing, J. P., "Potential Flow about Two-Dimensional Airfoils," Rept. LB31946, Dec. 1965, McDonnell-Douglas Corp.

[2] McCullough, G. B. and Gault, D. E., "Examples of Three Representative Types of Airfoil-Section Stall at Low Speed," TN-2502, Sept. 1951, NACA.

[3] Roshko, A., "A New Hodograph for Free Streamline Theory," TN-3168, July 1954, NACA.

[4] Hildebrand, F. B., *Advanced Calculus for Applications*, Prentice-Hall, Englewood Cliffs, N.J., 1963, pp. 574–584, 362–365.

[5] Kuethe, A. M. and Schetzer, J. D., *Foundations of Aerodynamics*, 2nd ed., Wiley, New York, 1959, pp. 64–69.

[6] Jones, B. M., "An Experimental Study of the Stalling of Wings," RM 1588, Dec. 1933, Aeronautical Research Council.

Optimum Climb Trajectories at Constant Lift Coefficient

R. H. Andrews*
Northrop Corporation, Hawthorne, Calif.

For many years, it has been possible to calculate aircraft minimum-time-to-climb trajectories by use of the calculus of variations. The resulting flight paths, however, typically show a continual variation in aerodynamic and control parameters from one time point to the next. Consequently, it is always very difficult, if not impossible, for a human pilot to duplicate this optimal path. Usually the best that can be done is to try to fly the trajectory in a series of separate segments.

It has now been found that if an aircraft is flown throughout the climb at a constant lift coefficient, a minimum-time trajectory can be closely approximated.

Figure 1 shows the performance of a typical fighter-type aircraft in a climb from 25,000 to 46,000 ft. The optimum

Received May 26, 1969.

* Senior Engineer, Aerodynamics Research Branch, Aircraft Division. Member AIAA.

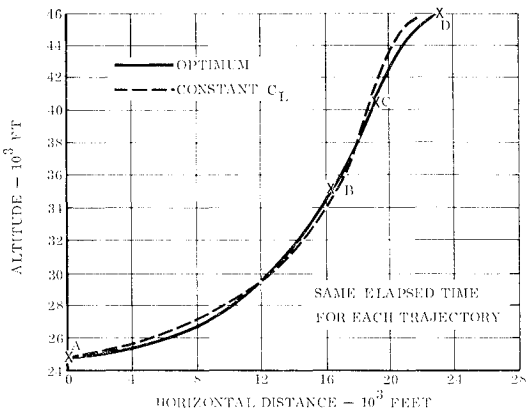

Fig. 1 Climb comparisons, aircraft no. 1.

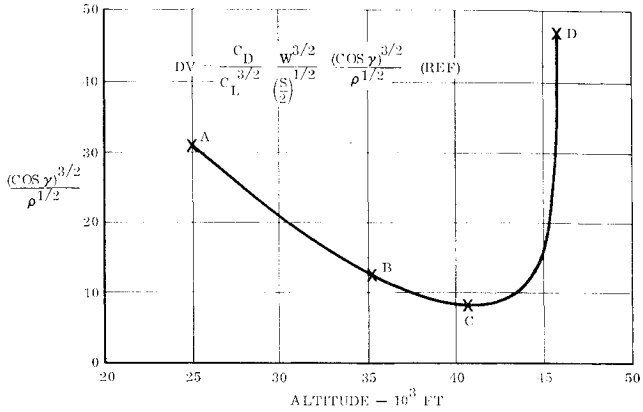

Fig. 3 Calculus of variations optimum climb.

flight path represents a minimum-time solution obtained by variational methods with two end-point constraints: the final altitude and a final flight-path angle of zero degrees. As can be seen, this optimum path can be closely approximated (in the same elapsed time) by holding the lift coefficient constant throughout the climb.

Figure 2 shows a climb from 2000 to 30,000 ft by another aircraft with a different T/W ratio. In this case, the constant C_L trajectory has a slightly different shape from that of the optimum. However, the total elapsed time and the end-point conditions closely approximate those of the variational solution.

The reasons why a constant C_L climb will behave in this manner are as follows. The ability to climb at any time point is determined by the excess of horsepower available over horsepower required at that particular point. The greater the excess power, the higher the climb rate will be. As a result, it can be shown that an optimum climb results from minimum horsepower required considered over the entire time span of the trajectory.

The expression for horsepower required is DV, or drag times velocity,

$$DV = C_D(\rho/2)SV^2(V) = C_D(\rho/2)SV^3 \tag{1}$$

In a climb, $L = W\cos\gamma$, where γ = the flight-path angle,

$$\therefore L = C_L(\rho/2)SV^2 = W\cos\gamma$$

or

$$V^2 = W\cos\gamma/C_L(\rho/2)S \tag{2}$$

Substituting (2) in (1),

$$DV = \left(\frac{C_D}{C_L^{3/2}}\right)\frac{W^{3/2}}{(S/2)^{1/2}}\frac{(\cos\gamma)^{3/2}}{\rho^{1/2}} \tag{3}$$

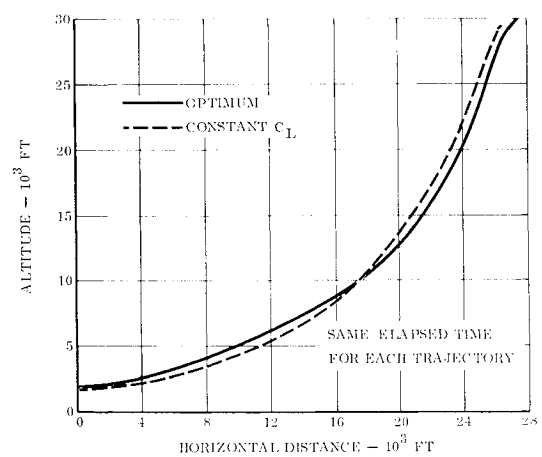

Fig. 2 Climb comparisons, aircraft no. 2.

Power is the rate of doing work. Therefore the integral of Eq. (3) over the time duration of the climb represents the total work performed during this period. When the total work performed is the least, the climb will be very close to the optimum.

The optimum (calculus of variations) trajectories shown in Figs. 1 and 2 must, and do, obey this physical law. Although these optimums were obtained by variational methods, the numerical integration of the DV's along the time span of the flight path will show a minimum total value, as compared with other possible climb trajectories reaching the same end points.

If a climb is steeper than the optimum, the DV total will be higher. This is because C_L, and therefore C_D, will be larger at the low altitudes where both air density and aircraft velocity are the greatest. A climb that is too shallow will also show a higher DV total, because aircraft velocity and the resulting drag will be higher throughout the climb. It is at the optimum flight path that the sum of the DV's will be least at the given end points of the trajectory. It will now be shown that the DV equation, Eq. (3), can be approximated by a linear function throughout the time span of an optimum climb.

In Fig. 3, the last term on the right side of Eq. (3) is shown plotted against altitude for the optimum (calculus of variations) climb that is shown in Fig. 1. Points A, B, C, and D correspond to the same time points in Figs. 1 and 3.

From the aircraft equations of motion,

$$\dot\gamma = (g/v)[n\cos\phi - \cos\gamma] \tag{4}$$

$$n = (L + T\sin\alpha)/W \tag{5}$$

The bank angle ϕ is zero and $T\sin\alpha$ is small relative to L, $\therefore n \cong L/W$ and

$$\dot\gamma \cong (g/v)[L/W - \cos\gamma]$$
$$L = C_L(\rho/2)SV^2 \tag{6}$$

$$\therefore \dot\gamma \cong g[C_L(\rho/2)SV/W - \cos\gamma/V] \tag{7}$$

The quantity which has the most effect on the magnitude and sign of $\dot\gamma$, in Eq. (7), is the velocity V. This parameter appears in both terms on the right side of the equation. Initially, with a high value of V, the first term will be larger than the second and $\dot\gamma$ will be positive. As the velocity decreases, the two terms approach each other in magnitude and $\dot\gamma$ finally becomes zero. This is the point B in Figs. 1 and 3. As shown in Fig. 3, the quantity $(\cos\gamma)^{3/2}/\rho^{1/2}$ is essentially linear in region A-B.

In the region B-C in Figs. 1 and 3, the flight-path angle has reached a steady-state value with $\dot\gamma$ approximately zero. Figure 3 shows the quantity $(\cos\gamma)^{3/2}/\rho^{1/2}$ again as essentially linear, but with a slightly different slope.

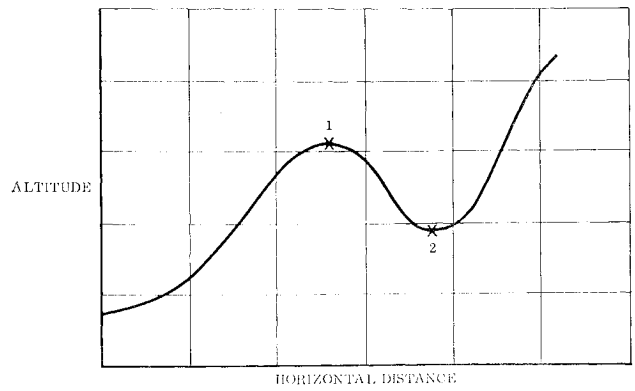

Fig. 4 Typical calculus of variations intercept problem solution.

As velocity V continues to decrease, $\dot{\gamma}$ becomes negative in Eq. (7) and the nose of the aircraft starts to fall toward the horizon. This is the region C-D in Fig. 3, and as can be seen is decidedly nonlinear.

However, about 98% of the total DV of the climb has been attained when point C is reached. Nearly 65% of the total time to climb has elapsed, and the aircraft is now moving so slowly in thin air (relative to the initial conditions) that the contribution of C-D to the total DV summation is negligible.

It can be seen from Fig. 3 that the segment A-B-C can be approximated by a straight line. As shown previously, this represents about 98% of the DV total in an optimum (calculus of variations) climb. Therefore, the term $(\cos\gamma)^{\frac{3}{2}}/\rho^{1/2}$ in Eq. (3) can be considered to be a linear function.

The term $W^{3/2}/(S/2)^{1/2}$ is roughly constant. Therefore, if a certain value of C_L is chosen and held constant throughout the climb, the term $C_D/C_L^{3/2}$ can be minimized for the whole trajectory. This will result in a minimum total DV, and the climb will approximate the optimum.

It can be shown[1] that where $C_L^{3/2}/C_D$ is maximum, the least power required results. Therefore, theoretically, the value of C_L to be held constant is one which will give a maximum value of this parameter. The trajectory in Fig. 1 resulted from flying approximately in this manner.

There is, however, another consideration. The equation governing the flight-path angle is

$$\sin\alpha = [T - D - (W/g)\dot{V}]/W \qquad (8)$$

Starting at a low altitude, as in Fig. 2, the T/W ratio is quite high. Flying at maximum $C_L^{3/2}/C_D$ would result in too steep a climb. In this case, a lower value of constant C_L must be selected.

Regardless of altitude, however, if the proper value of C_L is chosen and held constant throughout the climb, a close approximation to the optimum solution will result.

Figure 4 shows a typical calculus of variations solution to a minimum-time-to-climb intercept problem. The usual "humps" in the optimum trajectory are shown at points 1 and 2. By holding C_L constant in the climb, these "humps" will automatically be duplicated as indicated in the preceding analysis of Eq. (7). This will result in a close approximation to the variational solution.

The foregoing analysis is of minimum-time-to-climb trajectories in which there are two end-point constraints: final altitude and flight-path angle. A third constraint might be added in the form of a desired final aircraft velocity. This type of trajectory, also, can be closely duplicated by flying at a certain constant C_L. The reasoning for this case is similar to that given above.

The actual value of C_L to be held constant in any climb must be determined by trial and error, and will vary with different altitudes and end-point constraints. The calculus of variations solution must first be obtained. Then computer runs can be made using different values of constant C_L until the variational solution is most closely duplicated.

The foregoing method is based on flying the climb trajectories at a constant lift coefficient. However, approximately the same results can be obtained by flying at a constant angle of attack. Since the required "alpha" is always quite small, there is little Mach number dependence and the computed results are comparable.

Since aircraft angle-of-attack meters are now available, this might be a new way to fly minimum-time-to-climb trajectories for intercept missions, airline work, etc.

Reference

[1] Jones, B., *Elements of Practical Aerodynamics*, 4th ed., Wiley, New York, 1950, pp. 131–132.

Effects of an Isobaric, Inhomogeneous Atmosphere on Sonic Boom

W. F. Merzkirch*
Ernst-Mach-Institut, Freiburg i. Br., Germany

THE intensity of the sonic boom recorded at the ground depends, among other parameters, on the atmospheric conditions between the aircraft's flight path and the ground. Therefore a general analysis of the sonic boom should include gradients of atmospheric pressure, temperature, and wind. A special case is given if the atmosphere can be regarded to be isobaric, i.e., if there is no vertical pressure gradient; this results in an important simplification of the governing equations. The real atmosphere, however, is far from being isobaric, and the assumption is not justified unless one considers only a relatively thin atmospheric layer where the pressure gradient due to gravity is negligibly small.

The latter applies, for example, to the atmospheric surface layer near the ground, the vertical extension of which being much smaller than the usual flight heights of supersonic aircraft. On the other hand, this layer is dominated by influences of weather and exhibits noticeable changes in temperature and wind; hence the question arises how these variations may affect the intensity of the sonic boom. Several authors[1–3] have studied this problem assuming a constant pressure atmosphere with vertical temperature gradient and wind parallel to the flight direction. Since the sonic boom travels a long distance before it reaches this "weather layer" near the ground, its strength has weakened considerably. Pan[3] therefore assumes that the boom can be described here by a simple compression wave; he also treats, like Auriol et al.,[2] the two-dimensional case. Changing the coordinate system by superposing the velocity of the plane, one has a stationary compression wave that is exposed to a parallel supersonic flow with constant static pressure, but with a certain Mach number profile. This change in Mach number is generated either by the temperature gradient (change of the velocity of sound) or by a wind parallel to the flight direction (change of the flow velocity).

Pan's calculation is based on a compression-wave/vortex sheet interaction concept; the freestream (in the new coordinate system) is divided into n uniform sheets parallel to the ground, each of them having a constant Mach number M_i $(i = 1, 2, \ldots n)$. The interaction of the transmitted compression wave with the contact surfaces separating the individual stream sheets is then calculated step by step until the

Received May 21, 1969.
* Research Scientist. Member AIAA.